RESEARCH ARTICLE

Analysis of Stiffness Change of Panc-1 Cells Pre/Post Epithelial-mesenchymal Transition Induced by TGF-β

Xi Wan[1], Parminder Kaur[2], Yanping Cao[3], Yifan Zhu[3*], Yonggang Ma[1*]

[1]College of Pharmacy, Nankai University, Haihe Education Park, Tianjin, China

[2]Department of Physics, North Carolina State University, Raleigh, North Carolina, United States of America

[3]International Joint Laboratory for Cell Medical Engineering of Henan Province, Henan University Huaihe Hospital, Kaifeng, Henan Province, China

ABSTRACT

Pancreatic Ductal Adenocarcinoma (PDAC) is a disease with high mortality rates due to metastasis. Epithelial-Mesenchymal Transition (EMT) is correlated with metastasis and drug resistance in PDAC. Therefore, elucidating the changes in cellular characteristics in PDAC before and after EMT is essential to understand EMT in PDAC cells and to develop novel therapeutic methods for PDAC.

The human PDAC cell line Panc-1 was used to measure cell stiffness before and after EMT induction by TGF-β. EMT biomarker expression levels were measured to identify cell status using real-time PCR, immune cytochemistry. Changes in cell stiffness before and after EMT were investigated by Atomic Force Microscope with Young's modulus. Cell size was determined by image analysis. Cellular lipids were examined. Expression levels of lamin A, the gene associated with cell stiffness, were quantified by real-time PCR.

After induced EMT, PDAC cells were stiffer with larger cell sizes than before EMT. The expression levels of cytoskeletal proteins did not change significantly, but lamin A expression was significantly reduced after EMT. The amount of polyunsaturated fatty acids in the cell membrane increased, while monounsaturated fatty acids decreased. We reported the changes of cell stiffness and other biological characteristics in PDAC cells after EMT.

Cell stiffness was determined by multiple factors before and after EMT. These results provide new directions for understanding EMT in PDAC, which is critical for developing new therapies for PDAC.

Keywords: Atom force microscope; Cell stiffness; Epithelial-mesenchymal transition; Fatty acid; Pancreatic ductal adenocarcinoma

Abbreviations: PDAC: Pancreatic Ductal Adenocarcinoma; EMT: Epithelial-Mesenchymal Transition; AFM: Atom Force Microscope; FA: Fatty Acid; BHT: 2, 6-Di-tert-Butyl-4-Methylphenol; SFA: Saturated Fatty Acids; UFA: Unsaturated Fatty Acids; MUFA: Monounsaturated Fatty Acids; PUFA: Polyunsaturated Fatty Acids

INTRODUCTION

PDAC is one of the most deadly cancers [1]. In PDAC, which has a poor survival rate, metastasis is a significant prognostic factor and contributes most to cancer-related death [2]. During metastasis, transforming cancer cells migrate from their primary site to a secondary site, which is a multifactorial process requiring cytoskeletal and membrane reorganization [3]. This process is closely related to the mechanotype of the cell [4].

EMT is one of the well-known metastasis mechanisms, which represents a series of changes including cell shape, cell-cell junctions, cytoskeletal organization, and gene expression etc. EMT is correlated with more aggressive and advanced metastasis of PDAC [5]. Deeper insight into the cellular features in EMT might be helpful to address the challenges of PDAC.

Cell stiffness is an important cellular mechanical factor in metastasis [6]. Cell stiffness is primarily determined by the intracellular cytoskeleton and plasma membrane [7].

It is well established that stiffer PDAC cells are more invasive than more compliant PDAC cells [8]. However, how PDAC cell stiffness changes after EMT transition has not been fully elucidated.

Received: 16-Jul-2025, Manuscript No IPP-25-22749; **Editor Assigned:** 18-Jul-2025, PreQC No IPP-25-22749 (PQ); **Reviewed:** 01-Aug-2025, QC No IPP-25-22749; **Revised:** 08-Aug-2025, Manuscript No IPP-25-22749 (R); **Published:** 15-Aug-2025, DOI: 10.35841/1590-8577-26.2.920

Correspondence Yifan Zhu

International Joint Laboratory for Cell Medical Engineering of Henan Province, Henan University Huaihe Hospital, Kaifeng, 475000, Henan Province, China

E-mail celltransplant@163.com

Yonggang Ma

College of Pharmacy, Nankai University, Haihe Education Park, Tianjin, 300353, China

E-mail mayonggang@nankai.edu.cn

Citation: Wan X, Kaur P, Cao Y, Zhu Y, Ma Y. Analysis of Stiffness Change of Panc-1 Cells Pre/Post Epithelial-mesenchymal Transition Induced by TGF-β. JOP. J Pancreas. (2025) 26:920.

In an attempt to understand the interaction of EMT and stiffness in PDAC, a human PDAC cell line (Panc-1) was induced into EMT by TGF-β at a defined concentration and time point to ensure a successful EMT transition. Cell stiffness before and after EMT was then assessed by AFM using Young's modulus as reported [8]. As vimentin, actin and lamin A are three key mechanoregulatory factors, their expression along with tubulin expression was checked by real-time PCR, while FA analysis was also measured in pre-EMT and induced EMT groups.

MATERIALS AND METHODS

Cell management

Solutions and reagents: DMEM culture medium and phosphate-buffered saline were purchased from Boster Biological Technology Co.Ltd (Wuhan, China). Fetal bovine serum was obtained from Zhejiang Tianhang Biotech (Hangzhou, China). TGF-β was purchased from Invitrogen (Carlsbad, CA, USA). RNeasy Mini kit and Omniscript RT Kit were purchased from Qiagen (Valencia, CA, USA). PrimeScript™ RT Reagent Kit was purchased from TaKaRa (Takara Bio Inc., Shiga, Japan). SYBR Green kit was obtained from Bio-Rad (Hercules, CA, USA). Primary antibodies for E-cadherin, cytokeratin, vimentin, alpha-SMA, lamin A, and secondary antibodies were purchased from Proteintech (Wuhan, China).

Cell culture: The human PDAC cell line Panc-1 was obtained from American Type Culture Collection (Manassas, VA, USA) and cultured in DMEM medium under 37°C, 5% CO_2 conditions. Cell passaging was performed at 80% cell confluence. Cells were termed as pre-EMT group and EMT group.

TGF-β induced EMT: TGF-β in concentration series (5 ng/mL, 10 ng/mL, 20 ng/mL) was added individually into Panc-1 culture dishes of EMT group. After 72 hours, the cells were harvested, and the mRNA expression of EMT biomarkers (E-cadherin, Cytokeratin, Vimentin, alpha-SMA) was tested by real-time PCR. The TGF-β concentration with the most different mRNA expression level after induced EMT compared with that in the pre-EMT group was used for further experiments.

Examination of gene expression levels: Expression levels of EMT biomarkers, vimentin, actin, tubulin and lamin A were determined by real-time PCR. Total RNA was isolated using an RNeasy Mini Kit. PrimeScript™ RT Reagent Kit was used for cDNA synthesis according to the manufacturer's instructions. Real-time PCR was performed using the LightCycler® 96 system (Roche Diagnostics, Basel, Switzerland) according to the manufacturer's instructions. The reaction mixture (20 μL) contained 5 μL cDNA of target gene, 0.5 μL upstream and downstream PCR primers (Table S1), 10 μL SYBR Green qPCR SuperMix and 4 μL ddH2O. The house-keeping gene Glyceraldehyde-3-Phosphate Dehydrogenase (GAPDH) was used for signal normalization. The amplification protocol included an initial denaturation step at 95°C for 2 minutes, followed by 40 cycles at 95°C for 15 s and 60°C for 32 seconds. The 2-ΔΔCt method was used to calculate the fold change in gene expression. Experiments were repeated at least 3 times.

Immune Cytochemistry (ICC) assay: After the culture medium was removed, adherent cells were directly fixed with 3% parafomaldehyde, permeabilized with 0.5% Triton X-100 (Sigma-Aldrich, USA), and then ICC was used according to the manufactures' instructions for individual primary and secondary antibodies of E-cadherin, Cytokeratin, Vimentin, and alpha-SMA. After counterstaining with Mayer's hematoxylin, the slides were examined microscopically (Olympus culture microscope, model CKX53).

Measurement of cell stiffness: AFM studies of adhered Panc-1 cells were performed as reported. Briefly, before performing AFM force mapping measurements, the prepared adherent cells were washed with 1X PBS buffer. Cells were imaged using an inverted microscope (TiE, Nikon) as the AFM base (PlanFluor × 20, 0.5 NA Objective).

The AFM experiments were carried out on live cells. An AFM-3D-BIO AFM (Asylum Research) was used for force mapping with a BioLever mini-BL-AC40TS (Silicon Nitride cantilever, f=110 kHz, k=0.09 N/m). Force maps were fitted using the Hertz model to calculate Young's modulus for each area on the cell surface, assuming a Poisson's ratio of 0.4. Cells (N=10 for each condition) were analyzed with a 6 × 6 force map in a 10 μm × 10 μm area, in the cytoplasmic region on two opposite sides of the nucleus.

Measurement of cell size: Cells from the control and EMT groups were photographed using an Olympus culture microscope (model CKX53). Photographs were analyzed using ImageJ software.

Determination and analysis of cellular total fatty acids

Reagents: 37 fatty acid methyl esters mixture (Table S2), BHT, and acetyl chloride were purchased from Sigma-Aldrich (Sigma-Aldrich, Inc., USA). Heptadecanoic acid-D33 (C17:0-D33) was purchased from CDN (CDN Isotopes Inc., Canada). K_2CO_3 was purchased from SCRC (Sinopharm Chemical Reagent Co., Ltd., China). HPLC grade methanol and hexane were purchased from Thermo Fisher (Thermo Fisher Scientific Inc., USA).

Sample preparation: Cell pellets were re-suspended in 0.5 mL pre-cooled methanol and subjected to three freeze-thaw cycles before sonication in an ice bath for 15 minutes (cycles: 1 minute pulse followed by 1 minute pause). Aliquots (20 μL) were mixed with 10 μL of the internal standard (0.2 mg/mL of C17:0-D33, 0.4 mg/mL

Citation: Wan X, Kaur P, Cao Y, Zhu Y, Ma Y. Analysis of Stiffness Change of Panc-1 Cells Pre/Post Epithelial-mesenchymal Transition Induced by TGF-β. JOP. J Pancreas. (2025) 26:920.

of BHT in methanol) and 200 µL of methanol-hexane (4:1, v/v). The tubes were gently vortexed, and then placed in a home-made liquid nitrogen bath for 10 minutes. 20 µL of acetyl chloride was slowly added to the tubes and then kept in the dark at room temperature for 24 hours. 0.5 mL of 6% K_2CO_3 solution was slowly added to stop the reaction and the mixture was neutralize in an ice bath. After 50 µL of hexane was added to extract fatty acid methyl esters, and the tubes were briefly vortexed and then centrifuged (3000 rpm, 10 minutes), the top layer was collected and transferred to a sample vial for GC analysis.

GC-FID/MS analysis: The GC-FID/MS consisted of an Agilent 7890B gas chromatograph coupled to an Agilent 5977B mass spectrometer with a flame ionization detector (Agilent Technologies, USA). An Agilent DB-225 capillary GC column (10 m, 0.1 mm ID, 0.1 µm film thickness) was employed with a sample injection volume of 2 µL and a splitter (1:20). Helium gas was used as carrier gas and nitrogen gas as make-up gas. The injection port and detector temperatures were both set at 230°C.

The column temperature was set at 55°C for 1 minute and then increased to 205°C with a rate at 30°C/min. The column temperature was then kept at 205°C for 3 minutes and increased to 230°C (5°C/min) and held at 230°C for 1 minute. The MS spectra were acquired with the EI voltage of 70 eV and the m/z range of 45-450.

Data pre-processing: Peak identification and peak area integration were performed using MassHunter Workstation software (Agilent, version B.08.00). Methylated fatty acids were identified by comparison with a chromatogram from a mixture of known standards (Table S2) and further confirmed by their mass spectral data.

The concentration of each fatty acid was calculated from their FID data relative to the internal standard. The molar percentages were calculated from the above results for SFA, UFA, MUFA and PUFA.

Statistical analysis

All results are expressed as mean ± SD. Differences between groups were evaluated by analysis of variance, and post hoc analysis was performed by the Tukey-Kramer test. The p values less than 0.05 were considered statistically significant.

RESULTS

Verifying TGF-β induced EMT

Cells in EMT status should express high levels of mesenchymal biomarkers vimentin and alpha-SMA and low levels of epithelial biomarkers E-cadherin and cytokeratin expression. The results of Real-time PCR (Figure S1) and ICC (Figure S2) indicated that TGF-β at 10 ng/mL for 72 hours can successfully induce EMT in Panc-1 cells.

Measurement of cell stiffness

Cell stiffness of the control and EMT groups was measured using atomic force microscopy and Young's modulus. The results showed that the cell stiffness of the EMT group was significantly higher compared to the pre-EMT group (Figure 1A and Figure S3).

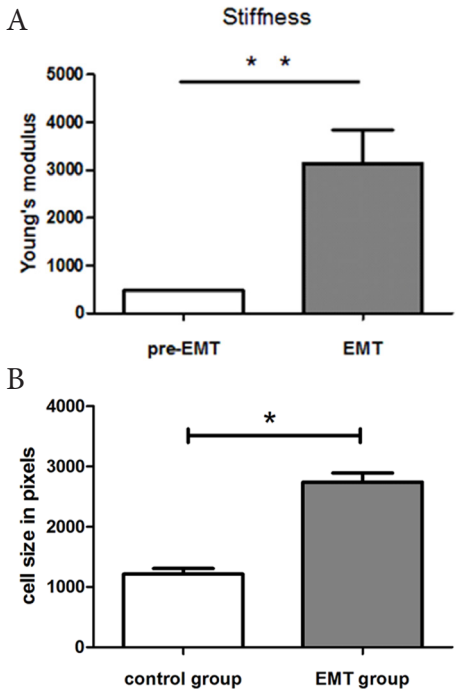

Figure 1. Cell stiffness and volume were significantly increased ($p<0.05$). (A) Cellular stiffness of EMT group was significantly higher than control. (B) Cellular volume of EMT group was significantly larger than control.

Citation: Wan X, Kaur P, Cao Y, Zhu Y, Ma Y. Analysis of Stiffness Change of Panc-1 Cells Pre/Post Epithelial-mesenchymal Transition Induced by TGF-β. JOP. J Pancreas. (2025) 26:920.

Measurement of cell size

The difference in cell size between control and EMT groups was also examined. The results showed that cell size was significantly increased after induced EMT compared to cells cultured for the same time in the control group (Figure 1B).

Analysis of expression of cytoskeleton proteins

The expression of cytoskeletal proteins and lamin A at the mRNA level was analyzed by the real-time PCR. Results showed that after cell cultivation with TGF-β at 10 ng/mL for 72 hours EMT was induced. However, there were no significant changes in the expression of cytoskeletal proteins (Figure 2A and 2B), while the expression of lamin A was significantly down-regulated compared with that in pre-EMT group (Figure 2C).

Changes in the fatty acids

Analysis of the intracellular total FA metabolism in pre/post-EMT cells showed that the level of total FA keeps stable in two groups (Figure 3A), and the proportion of SFA and UFA in pre-EMT and EMT groups also stays equable (Figure 3B and 3C). However, the level of MUFA is significantly decreased in EMT group (Figure 3D) while the PUFA shows an elevated level without significance in EMT group (Figure 3E).

While the total SFA level remains unaltered in the EMT group, its C14:0 subtype exhibits a markedly diminished level (Figure 4A). Similarly, for PUFA, there are subtypes C20:3n6 and C20:4n6 that are significantly up-regulated in the EMT group, respectively, while the total PUFA level remains stable in the EMT group (Figure 4B and 4C). In the case of MUFA, the significantly depressed level observed in the EMT group is largely attributable to the markedly reduced levels of the subtypes C17:1 and C20:1, respectively (Figure 4D and 4E). Additionally, a notable elevation in the ratio of SFA to MUFA was discerned in the EMT group (Figure 4F).

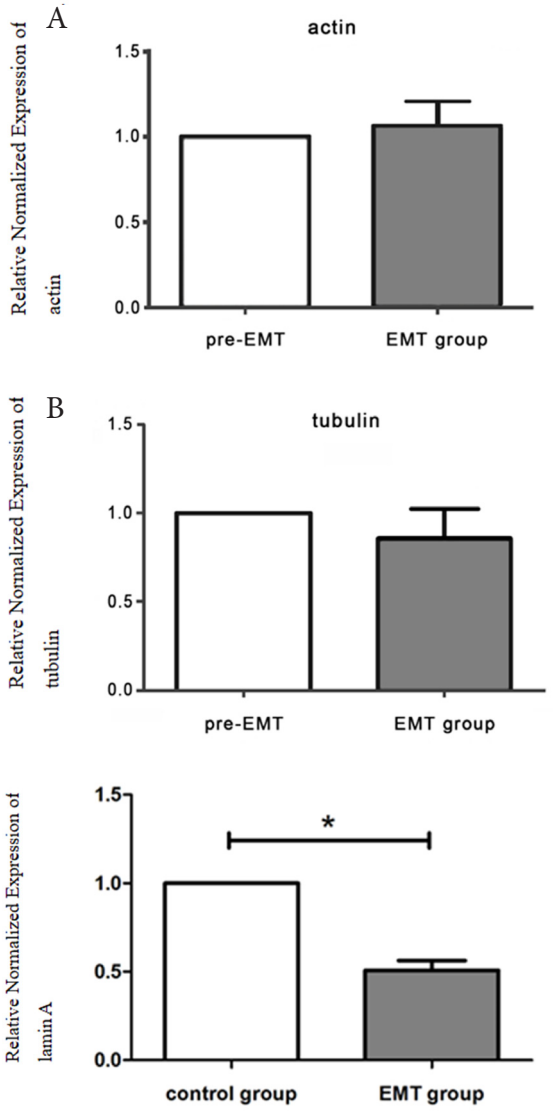

Figure 2. The mRNA levels of actin (A) and tubulin (B) are stable, whereas lamin A was significantly down regulated in EMT group ($p<0.05$).

Citation: Wan X, Kaur P, Cao Y, Zhu Y, Ma Y. Analysis of Stiffness Change of Panc-1 Cells Pre/Post Epithelial-mesenchymal Transition Induced by TGF-β. JOP. J Pancreas. (2025) 26:920.

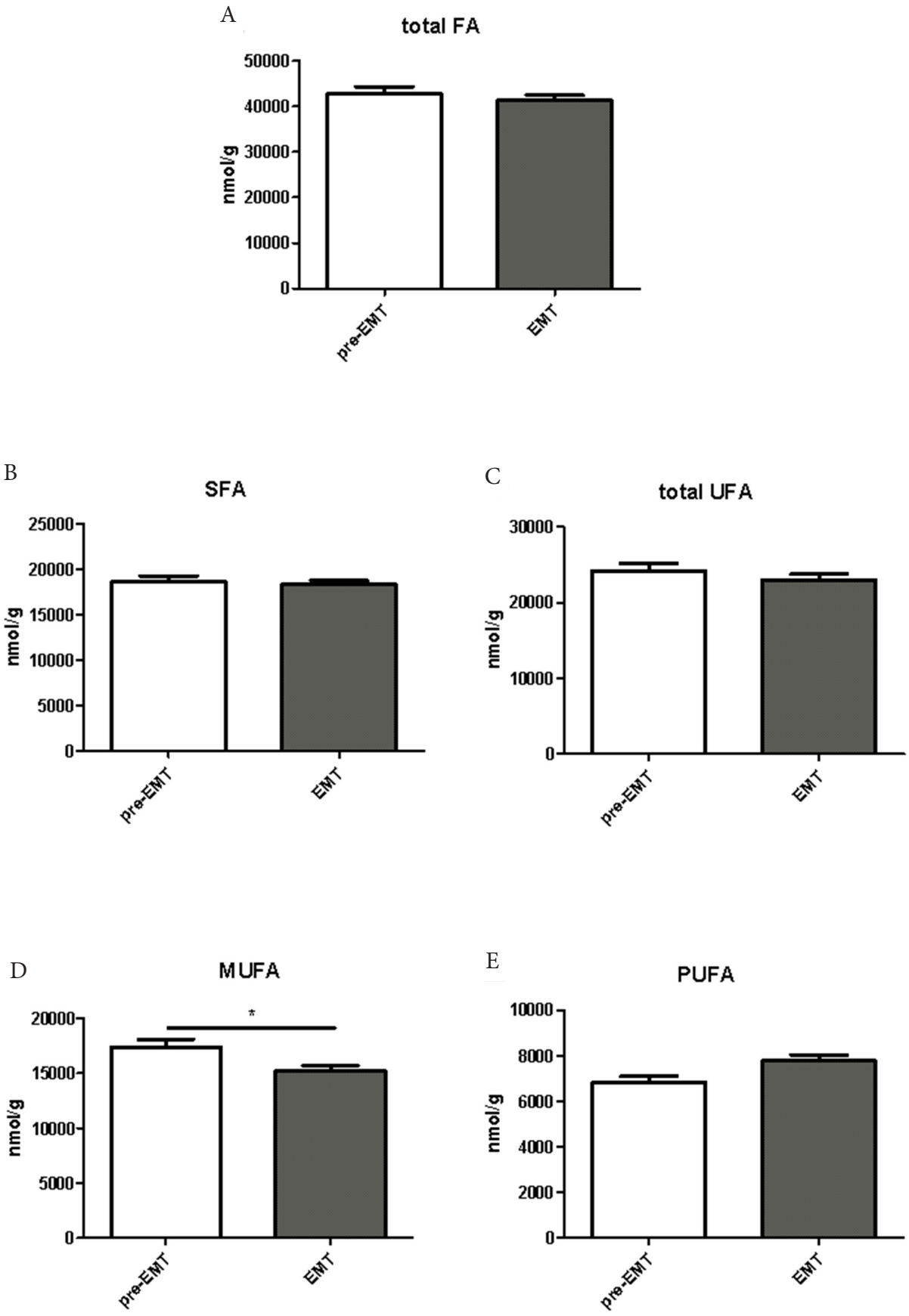

Figure 3. Levels of total FA, SFA, UFA, MUFA, and PUFA in pre-EMT and EMT groups. (A, B, C, and E) The levels of total FA, SFA, UFA, and PUFA did not alter significantly; (D) The level of MUFA decreased significantly (*p<0.05).

Citation: Wan X, Kaur P, Cao Y, Zhu Y, Ma Y. Analysis of Stiffness Change of Panc-1 Cells Pre/Post Epithelial-mesenchymal Transition Induced by TGF-β. JOP. J Pancreas. (2025) 26:920.

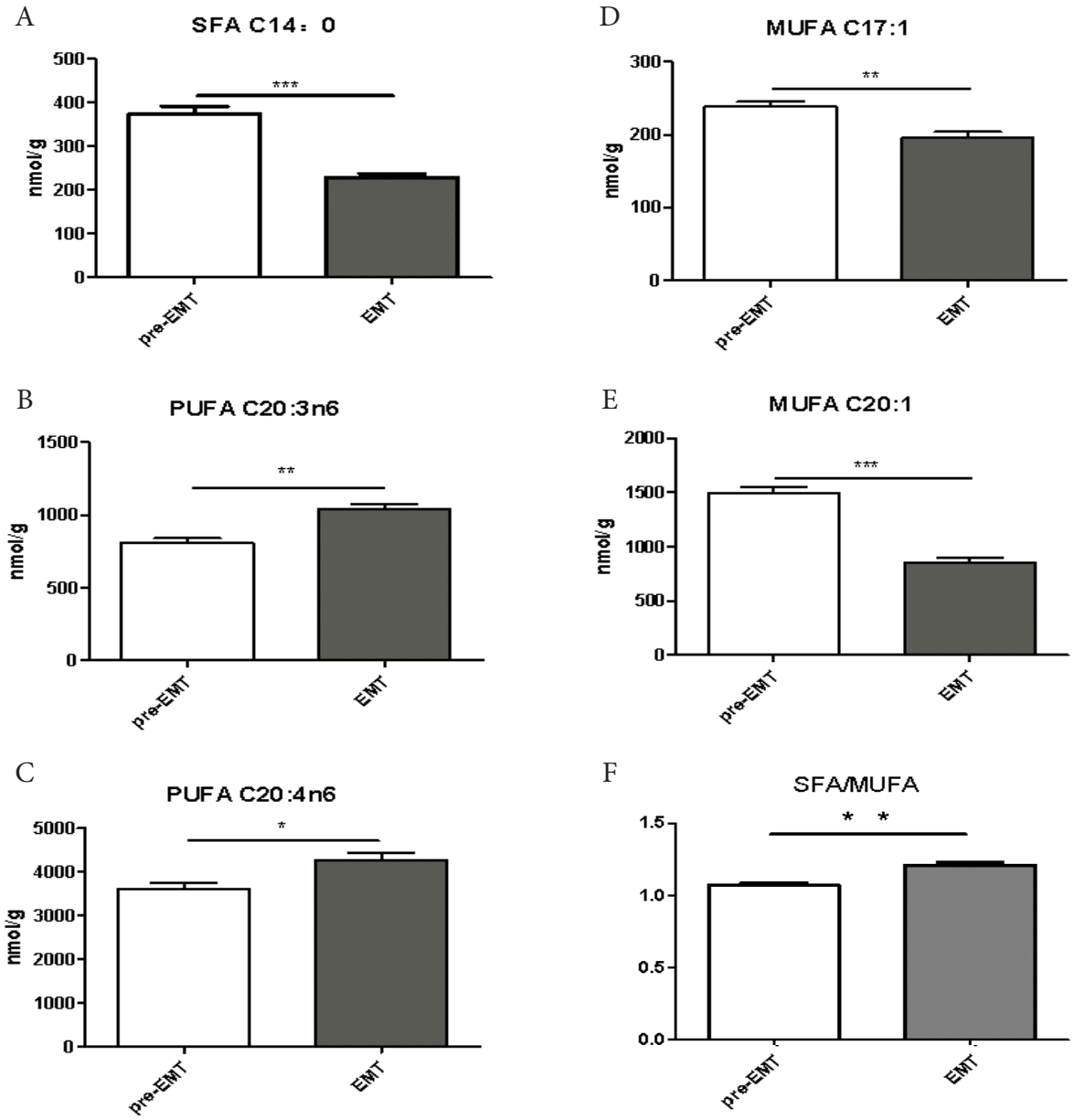

Figure 4. Significant changes in the subtypes of fatty acids were observed in SFAs, PUFAs, and MUFAs. (A) There is a notable decline in the level of SFA C14:0. (B,C) PUFAs C20:3n6 and C20:4n6 exhibited a notable increase in the EMT group. (D,E) MUFAs C17:1 and C20:1 exhibited a notable increase (*p<0.05, **p<0.01, ***p<0.001). (F) The ratio of SFA to MUFA significantly elevated in EMT groups. (*p<0.05, **p<0.01, ***p<0.001).

DISCUSSION

Metastasis is the major contributor to cancer-related death in poor-survival PDAC [2]. EMT is correlated with a more aggressive phenotype and advanced metastasis of PDAC [5]. Moreover, stiffer PDAC cells are more invasive than more compliant PDAC cells [8]. With the achievement above, it is reasonable to assume that PDAC cells in EMT might be stiffer being of more metastasis than that in pre-EMT. In our study, PDAC cell line Panc-1 was successfully induced into EMT by TGF-β, AFM investigation with Young's modulus shows that Panc-1 cells in EMT group is significantly stiffer than that in pre-EMT group. These data provide additional insight into PDAC EMT, which correlates with advanced metastasis.

It is well known that cell stiffness is mainly determined by the intracellular cytoskeleton and plasma membrane [7]. Our results showed that the expression of actin and tubulin were stable in EMT group, while the expression of vimentin and lamin A was significantly up and down-regulated respectively, in the EMT group in compared with the pre-EMT group.

Actin-based microfilaments, tubulin-based microtubules and intermediate filaments (including vimentin) comprise

Citation: Wan X, Kaur P, Cao Y, Zhu Y, Ma Y. Analysis of Stiffness Change of Panc-1 Cells Pre/Post Epithelial-mesenchymal Transition Induced by TGF-β. JOP. J Pancreas. (2025) 26:920.

the cytoskeleton [9]. Numerous studies have convincingly concluded that actin is the major contributor to cellular stiffness, microtubules play a minimal role, and intermediate filaments act as a supporting role in regulating intracellular mechanics [10]. Factors in actin regulation of cell stiffness could be the expression of the actin associated protein Tropomyosin (Tpm), MAPK signaling and the bundling model of actin filament [11].

Actin-based microfilament performs multiple functions in cytokinesis, cell motility, mechanical stability, etc. [12]. Through PDAC EMT, a remodeling of the actin-based microfilament is induced under multiple signaling pathway such as TGF-β, Wnt, receptor tyrosine kinase, Notch and Hedgehog signalling pathways [13]. During the remodeling process, actin monomers polymerize in response to signaling cascades with the help of actin-binding proteins [14]. Taken together with the results of our study, it is clear that there are no significant changes in actin expression along with actin remodeling after EMT, implying that remodeling, not expression, plays a key role in cellular stiffness changes.

Depressed vimentin expression can lead to reorganization of cytoskeletons, weakened focal adhesion and impaired mechanical strength due to reduced cell stiffness and contractile force *via* advanced β1-integrin expression and absence of E-cadherin junction [15]. On the other hand, vimentin overexpression can increase cell stiffness associated with a more aggressive status as being in EMT [16], which is represented by significantly up-regulated vimentin synchronizing a significantly increasing cell stiffness in EMT group in our study.

The cytoskeleton functions in cytoplasma, lamin A works intranuclearly. Structurally, there are four lamin proteins (A, C, B1, B2) [17], which interact to form a polymeric network in the nuclear periphery over the inner nuclear membrane, the lamina, which is responsible for nuclear stability and chromatin organization [18]. There are paradoxical results from individual studies of lamin A expression in cancer cells, and both lower and higher levels of lamin A both might be beneficial to cancer cells [19]. Rowat's research found that increased lamin A expression was associated with higher Young's modulus for cell stiffness and more invasive potential [8].

In our study, the results showed that increased Young's modulus was associated with significantly reduced lamin A expression after induced EMT was exposed. It has been shown that lower lamin A expression can result in cells having more deformability in passing through narrow gaps [20], which meets the requirements for more migratory ability in EMT.

It has been popular that biological membrane is heterogeneous composed of lipid and protein mixtures termed as lipid domains [21], and membrane lipid-protein domains have been studied as functional unit as membrane rafts, which is composed of sphingolipid, cholesterol and bound signaling proteins such as Src-family kinases and Glycosylphosphatidylinositol (GPI)-anchored proteins suggesting its function in signaling pathway [22].

Fatty acids are carboxylic acids, and based on saturated and unsaturated hydrocarbon chains, fatty acids can be classified into saturated fatty acids and unsaturated fatty acids including monounsaturated fatty acids, and polyunsaturated fatty acids [23].

The endoplasmic reticulum enzyme stearoyl-CoA desaturase 1 catalyzes SFA to the biosynthesis of MUFA. In our study, of the stiffer cells in the EMT group, the total FA and the proportion of SFA and UFA remained stable in two groups, while the molar percentages of PUFA and MUFA were significantly increased and decreased respectively [24].

Due to the significantly reduced MUFA level, the ratio of intracellular SFA to MUFA (SFA/MUFA) is significantly elevated in EMT group compared to the pre-EMT group. The stable SFA and a reduced MUFA levels imply (1) a reduced MUFA biosynthesis, (2) lower membrane fluidity as in the gel phase after induced EMT. PUFA can increase membrane fluidity and decrease cell stiffness [25].

Its mechanism might be (1) the more cholesterol in the membrane, the less fluidity, the more rigidity, the less deformability and the thicker the membrane is, thus implying a higher cellular stiffness [26], due to the interaction between cholesterol and SFA resulting in a closer packing order of the membrane phospholipid with SFA tails [27]; (2) conversely, as an aversion to cholesterol, PUFA and cholesterol displace each other, forming lateral lipid segregation of PUFA-rich/sterol-poor and PUFA-poor/sterol-rich regions [28]. The elevated PUFA levels may result in a more heterogeneous membrane consisting of more PUFA-rich/sterol-poor domains and less PUFA-poor/sterol-rich domains in EMT.

CONCLUSION

The co-occurrence of elevated SFA/MUFA increasing cell stiffness and elevated PUFA decreasing cell stiffness in the EMT group needs further investigation. One possibility is that the cytoskeleton is of more important than the cell membrane in regulating cell stiffness. Obviously, cellular stiffness is highly orchestrated by multi-factors of the cytoskeleton and membranes.

AUTHORS CONTRIBUTION

Xi Wang: Investigation, Formal analysis. Parminder Kaur: Investigation, Formal analysis, Methodology. Yanping Cao: Data curation. Yifan Zhu: Conceptualization, Funding acquisition, Project administration, Writing-original draft. Yonggang Ma: Conceptualization, Supervision, Writing-review and editing.

Citation: Wan X, Kaur P, Cao Y, Zhu Y, Ma Y. Analysis of Stiffness Change of Panc-1 Cells Pre/Post Epithelial-mesenchymal Transition Induced by TGF-β. JOP. J Pancreas. (2025) 26:920.

COMPETING INTEREST

The authors declare that they have no competing interests.

FUNDING

This work was supported by Project 162102410006, Department of Science and Technology of Henan Province, People's Republic of China.

REFERENCES

1. Werner J, Combs SE, Springfeld C, Hartwig W, Hackert T, et al. Advanced-stage pancreatic cancer: Therapy options. Nat Rev Clin Oncol. 2013;10(6):323-33.
2. Peixoto RD, Speers C, McGahan CE, Renouf DJ, Schaeffer DF, et al. Prognostic factors and sites of metastasis in unresectable locally advanced pancreatic cancer. Cancer Med. 2015;4(8):1171-7.
3. Fife CM, McCarroll JA, Kavallaris M. Movers and shakers: Cell cytoskeleton in cancer metastasis. Br J Pharmacol. 2014;171(24):5507-23.
4. Lee MH, Wu PH, Staunton JR, Ros R, Longmore GD, et al. Mismatch in mechanical and adhesive properties induces pulsating cancer cell migration in epithelial monolayer. Biophys J. 2012;102(12):2731-41.
5. Alderton GK. Tumour immunology: Give it a rest. Nat Rev Cancer. 2013;13(3):150.
6. Luo Q, Kuang D, Zhang B, Song G. Cell stiffness determined by atomic force microscopy and its correlation with cell motility. Biochim Biophys Acta. 2016;1860(9):1953-60.
7. Ayee MA, Levitan I. Paradoxical impact of cholesterol on lipid packing and cell stiffness. Front Biosci (Landmark Ed). 2016;21(6):1245-59.
8. Nguyen AV, Nyberg KD, Scott MB, Welsh AM, Nguyen AH, et al. Stiffness of pancreatic cancer cells is associated with increased invasive potential. Integr Biol (Camb). 2016;8(12):1232-45.
9. Preisner H, Habicht J, Garg SG, Gould SB. Intermediate filament protein evolution and protists. Cytoskeleton. 2018;75(6):231-43.
10. Seltmann K, Fritsch AW, Käs JA, Magin TM. Keratins significantly contribute to cell stiffness and impact invasive behavior. Proc Natl Acad Sci U S A. 2013;110(46):18507-12.
11. Rudzka DA, Spennati G, McGarry DJ, Chim YH, Neilson M, et al. Migration through physical constraints is enabled by MAPK-induced cell softening *via* actin cytoskeleton re-organization. J Cell Sci. 2019;132(11):jcs224071.
12. Merino F, Pospich S, Raunser S. Towards a structural understanding of the remodeling of the actin cytoskeleton. Semin Cell Dev Biol. 2020:102:51-64.
13. Morris HT, Machesky LM. Actin cytoskeletal control during epithelial to mesenchymal transition: Focus on the pancreas and intestinal tract. Br J Cancer. 2015;112(4):613-20.
14. Kalwat MA, Thurmond DC. Signaling mechanisms of glucose-induced F-actin remodeling in pancreatic islet β cells. Exp Mol Med. 2013;45(8):e37.
15. Liu CY, Lin HH, Tang MJ, Wang YK. Vimentin contributes to epithelial-mesenchymal transition cancer cell mechanics by mediating cytoskeletal organization and focal adhesion maturation. Oncotarget. 2015;6(18):15966.
16. Brzozowa M, Wyrobiec G, Kołodziej I, Sitarski M, Matysiak N, et al. The aberrant overexpression of vimentin is linked to a more aggressive status in tumours of the gastrointestinal tract. Prz Gastroenterol. 2015;10(1):7-11.
17. Broers JL, Machiels BM, Kuijpers HJ, Smedts F, Van Den Kieboom R, et al. A-and B-type lamins are differentially expressed in normal human tissues. Histochem Cell Biol. 1997;107(6):505-17.
18. Broers JL, Hutchison CJ, Ramaekers FC. Laminopathies. J Pathol. 2004;204(4):478-88.
19. Matsumoto A, Hieda M, Yokoyama Y, Nishioka Y, Yoshidome K, et al. Global loss of a nuclear lamina component, lamin A/C, and LINC complex components SUN 1, SUN 2, and nesprin-2 in breast cancer. Cancer Med. 2015;4(10):1547-57.
20. Rowat AC, Jaalouk DE, Zwerger M, Ung WL, Eydelnant IA, et al. Nuclear envelope composition determines the ability of neutrophil-type cells to passage through micron-scale constrictions. J Biol Chem. 2013 Mar 22;288(12):8610-8.
21. Edidin M. The state of lipid rafts: From model membranes to cells. Annu Rev Biophys Biomol Struct. 2003;32(1):257-83.
22. Pike LJ. Rafts defined: A report on the keystone symposium on lipid rafts and cell function. J Lipid Res. 2006;47(7):1597-8.
23. Dobrzyn A, Ntambi JM. The role of stearoyl-CoA desaturase in the control of metabolism. Prostaglandins Leukot Essent Fatty Acids. 2005;73(1):35-41.
24. Matsuki H, Goto M, Tamai N. Membrane states of saturated glycerophospholipids: A thermodynamic study of bilayer phase transitions. Chem Pharm Bull (Tokyo). 2019;67(4):300-7.
25. Haghi M, Traini D, Wood LG, Oliver B, Young PM, et al. A 'soft spot'for drug transport: Modulation of cell stiffness using fatty acids and its impact on drug transport in lung model. J Mater Chem B. 2015;3(13):2583-9.
26. Roduit C, Van Der Goot FG, De Los Rios P, Yersin A, Steiner P, et al. Elastic membrane heterogeneity of living cells revealed by stiff nanoscale membrane domains. Biophys J. 2008;94(4):1521-32.
27. de Meyer F, Smit B. Effect of cholesterol on the structure of a phospholipid bilayer. Proc Natl Acad Sci U S A. 2009;106(10):3654-8.
28. Wassall SR, Stillwell W. Polyunsaturated fatty acid–cholesterol interactions: Domain formation in membranes. Biochim Biophys Acta. 2009;1788(1):24-32.

Citation: Wan X, Kaur P, Cao Y, Zhu Y, Ma Y. Analysis of Stiffness Change of Panc-1 Cells Pre/Post Epithelial-mesenchymal Transition Induced by TGF-β. JOP. J Pancreas. (2025) 26:920.